Molecular Weight Distributions and Chain-Stopping Events in the Free-Radical Polymerization of Methyl Methacrylate

Kim Y. van Berkel,[†] Gregory T. Russell,[†] and Robert G. Gilbert*[,‡]

Department of Chemistry, University of Canterbury, Private Bag 4800, Christchurch, New Zealand, and Key Centre for Polymer Colloids, Chemistry School F11, University of Sydney, Sydney, NSW 2006, Australia

Received September 24, 2004; Revised Manuscript Received February 13, 2005

ABSTRACT: The chain-stopping and radical-loss events in the seeded emulsion polymerization of methyl methacrylate are determined using information from the complete molecular weight distributions (MWDs) and rate behavior with initiation by γ radiolysis followed by removal from the radiation source ("γ relaxation"). The system follows "pseudo-bulk" kinetics, implying that the chain-stopping and radical-loss events are kinetically the same as in corresponding bulk and solution free-radical polymerizations. It was essential to take SEC (size-exclusion chromatography) band broadening into account when interpreting the MWDs. The MWDs are interpreted by plotting the log(instantaneous number MWD), which is expected to be linear from theory, but it is shown that broadening leads to an upward curvature, consistent with experimental observation in this and many other systems. It is proven that the slope of the true (unbroadened) log(instantaneous number MWD) can be found from that of the experimental (broadened) one by taking the slope at the peak of the SEC distribution. The experimental MWDs are found to be dominated by transfer to monomer. The γ-initiated rate data also show that radical loss is predominantly caused by the rapid diffusion of short radicals generated by transfer to monomer (i.e., the rate coefficient for termination is a function of those for transfer and primary radical termination). The transfer constant inferred from all these data ($k_{tr}/k_p = 2.3 \times 10^{-5}$) is in agreement with that obtained by alternative methods (Stickler, M.; Meyerhoff, G. *Makromol. Chem.* **1978**, *179*, 2729). All data can be acceptably modeled using diffusion theory to predict the rate coefficients of chain length dependent termination, with the few parameters adjusted to give the fit having values that are in good accord with the expected range.

Introduction

Quantitative information on chain-stopping and radical-loss events in free-radical polymerization can be obtained from two types of data: rates and molecular weight distributions. It is notoriously difficult to obtain consistent values of some of the rate coefficients involved, particularly those for termination, for which reasons have recently been discussed in the literature.[1] In essence, these difficulties arise because data interpretation must perforce involve a significant number of model-based assumptions. For termination this is rendered more complex because the microscopic rate coefficient for termination between two growing radicals depends on the degrees of polymerization of both radicals, and hence termination rates depend on radical concentrations and chain-length distributions, and hence implicitly on radical flux (initiator concentration, etc.). In addition, termination rate coefficients depend also on conversion (i.e., on polymer concentration), and as yet there are no benchmark data sets for termination rate coefficients at very low polymer concentrations. There are very few attempts in the literature to obtain such data at intermediate and high polymer concentrations, which are of considerable practical interest. Similarly, there is often a wide range of values reported in the literature for transfer constants to monomer. Knowledge of these rate coefficients, and especially physical understanding of these values and reliable models for predicting them, is of particular interest for commercial polymer production.

The present paper tackles this problem for methyl methacrylate (MMA), by combining data from a battery of techniques: molecular weight distributions, and rate data with initiation by both a thermal initiator (persulfate) and γ radiation. This last permits a study of the variation in rate as the reactor vessel is removed from the radiation source ("relaxation" mode), which provides data which are sensitive to radical loss events in the absence of a source of new radicals. The chosen polymerization method is emulsion polymerization. While emulsion polymerizations are inherently more complex than bulk and solution polymerizations, because of the existence of phase-change events (entry of radicals into, and desorption of radicals from, the latex particles), it happens that MMA (and quite a few other monomers) obey "pseudo-bulk" kinetics in most emulsion polymerizations: the kinetics and MWDs should be the same as in equivalent bulk and solution polymerizations. In this study, the complexities of particle formation are obviated by performing the polymerization in a preformed and well-characterized seed latex, ensuring that conditions are such that no new particles are formed.

There are two advantages of using emulsion polymerization for the present goals. (1) Rate data, including relaxation behavior, are readily and accurately obtained using dilatometry. (2) The preformed seed particles can be swollen with monomer as desired, and so data can be obtained for any desired polymer concentration (at or above that dictated by the equilibrium concentration of monomer in the particles). By operating in the presence of monomer droplets or controlled monomer feed, one can maintain a constant polymer concentration

[†] University of Canterbury.
[‡] University of Sydney.
* Corresponding author; email gilbert@chem.usyd.edu.au.

10.1021/ma048027g CCC: $30.25
Published on Web 03/19/2005

in the particles for an extended period. As monomer is consumed by polymerization inside a particle, monomer from droplets, or from a controlled feed, is transferred to the particles, to replace that which was consumed, to swell the newly formed polymer. One thus obtains a significant amount of polymer formed over conditions of constant polymer concentration. Molecular weight analysis of this polymer perhaps affords the closest approximation to truly instantaneous MWDs that can be obtained by free-radical polymerization.

It is noted that there are many studies of MMA rates and MWDs in the literature. What differentiates the present study is the combination of the use of γ relaxation data, which are specifically sensitive to radical loss events, and instantaneous MWD data, which are sensitive to chain-stopping events, to evolve a qualitative and quantitative picture of the dominant mechanisms controlling these two events.

Data Interpretation Methodology. The data comprise rates (including time-varying rates in γ relaxation mode) and molecular weight distributions. The objectives are to obtain rate coefficients for the chain-stopping events (transfer and termination) as a function of appropriate controllable variables, and to compare these with models. This comparison will not simply involve showing that one can obtain accord with the data using a complex model with many parameters whose values may be adjusted; rather, we use a minimum of model-based assumptions, infer rate parameters from the data and use these to test mechanistic hypotheses. The working hypothesis is that the termination rate coefficient depends on the degrees of polymerization of both terminating radicals: chain-length-dependent termination, which is implicit in the hypothesis[2] that termination between growing radicals is diffusion-controlled. For statistical reasons this in turn implies that for conventional systems (i.e., excluding "controlled" radical polymerizations[3,4] and systems with intermittent initiation), termination will be dominated by events involving a short mobile radical and a long immobile one (except perhaps at the very onset of polymerization).

Because termination rate coefficients depend on the degrees of polymerization of both chains, the type of data considered here will at best yield $\langle k_t \rangle$, the termination rate coefficient averaged over all chain lengths:

$$\langle k_t \rangle = \sum_{i=1}^{\infty} \sum_{j=1}^{\infty} k_t^{ij} \frac{n_i}{\bar{n}} \frac{n_j}{\bar{n}} \tag{1}$$

where i and j refer to the degrees of polymerization, $\bar{n}$ is the average number of radicals per particle, n_i is the average number per particle of radicals of degree of polymerization i ($\bar{n} = \sum n_i$), and k_t^{ij} is the termination rate coefficient between radicals of degree of polymerization i and j (eq 1 has been written in terms of $\bar{n}$, which is convenient for emulsion polymerizations; for bulk and solution systems, one has a corresponding expression in terms of radical concentrations). In an emulsion polymerization which obeys pseudo-bulk kinetics, intraparticle termination is the rate-controlling event for loss of radical activity, and the rate is given by[5]

$$\frac{d\bar{n}}{dt} = \rho - \frac{2\langle k_t \rangle \bar{n}^2}{N_A V_s} \tag{2}$$

where ρ the entry rate coefficient (the frequency of radicals which enter a particle), N_A the Avogadro constant and V_s the (monomer-)swollen volume of a latex particle. Hence an ideal relaxation experiment, where there is no source of new radicals, should yield $\langle k_t \rangle$ directly; in practice, there is usually a small amount of spontaneous radical generation in such systems,[6,7] which must be taken into account for accurate data interpretation. This methodology will be used to infer $\langle k_t \rangle$ from the relaxation rate data for a range of conditions.

Molecular weight distribution (MWD) data are usually obtained using size-exclusion chromatography (SEC). The theoretical interpretation of these distributions is most easily implemented in terms of the *number* MWD $P(M)$, which is the number distribution of chains with molecular weight M. $P(M)$ is related to the SEC distribution $w(\log M)$ by

$$w(\log M) = M^2 P(M) \tag{3}$$

which is the distribution that would be observed in an ideal SEC if the calibration curve were linear and there were no band broadening.[8−10] Both $w(\log M)$ and $P(M)$ have arbitrary normalization.

Interpretation of MWD data is best done using *instantaneous* MWDs, i.e., for polymer that is formed at a given polymer concentration and where the various controlling rate parameters do not change significantly, rather than the *cumulative* MWD over a large conversion range, where for example radical concentrations may change. Theory[9] suggests that the instantaneous $P(M)$ should have a simple exponential dependence on M. A common case is when chain stoppage is dominated by transfer to monomer and by termination, when one has[11]

$$P(M) = e^{-\Lambda M/M_0},\ \Lambda = \frac{k_{tr}}{k_p} + \frac{\langle k_t \rangle \bar{n}}{k_p [M]_p N_A V_s} \tag{4}$$

where M_0 is the molecular weight of monomer, V_s is the swollen volume of the particle, and k_{tr} and k_p are the rate coefficients for transfer (to monomer) and for propagation, respectively. Simulations[9] predict that ln P (obtained from the instantaneous SEC distribution using eq 3) should be linear in M except at very low molecular weights. Theory[9,11] also gives means whereby rate coefficients for termination and transfer can be obtained from the slope of such a plot, including its dependence on initiator concentration.

There are thus in principle two independent means of determining $\langle k_t \rangle$: relaxation rate data and MWD data. Given the notorious difficulty in obtaining meaningful and reliable values of termination rate coefficients,[12] accord between these two methods would suggest the reliability of the resulting $\langle k_t \rangle$. Values of the transfer rate coefficient k_{tr}, which can be inferred from MWD data under appropriate circumstances, can also be compared with those from more traditional methods such as a Mayo plot.

A major obstacle to the use of complete MWDs to infer rate coefficients is that the linearity expected in the instantaneous ln P is not generally observed. This surprising result, which has often been commented upon in the literature, will be discussed extensively in the present paper. It will be proved that a linear ln P combined with SEC band broadening can account for this nonlinearity. A new method will be deduced for

inferring the slope of the underlying linear ln P without the need for deconvoluting the SEC trace.

Finally, for the purposes of this paper it is essential to understand that even when dead chain formation is predominantly by transfer (i.e., when $\langle k_t \rangle$ is transfer-dominated), the rate of radical loss is still determined by termination. Under such circumstances a radical usually undergoes many cycles of growth and transfer before it terminates. Chain-length-dependent termination implies that a radical has a much faster rate coefficient for termination while it is small than while it is long. It is thus apparent that a transfer-dominated $\langle k_t \rangle$ must predominantly involve small radicals, and one might think of such termination as being a form of "primary radical termination".[13] Because under these circumstances the rate of generation of small radicals is governed by k_{tr}, it must play a central role in determining the value of $\langle k_t \rangle$.

Experimental Section

Seed Latex Preparation. Methyl methacrylate (Mitsubishi Rayon, stabilized with 4-methoxyphenol inhibitor) was passed through a column of basic alumina and distilled under reduced pressure (first and last 10% discarded) to remove inhibitor. The purified monomer was stored at 0 °C for no longer than 2 weeks before use. Aerosol MA-80 (AMA-80, sodium di(1,3-dimethylbutyl)sulfosuccinate, 80% solution in 2-propanol and water, Cytec) and sodium hydrogen carbonate (BDH AnalaR grade) were used without further purification. Potassium persulfate (KPS) (BDH AnalaR grade) was recrystallized from water before use. Water (700 g), AMA-80 (20.0 g), and $NaHCO_3$ (1.0 g) were heated to 60 °C. A small amount (50 cm^3) of water was retained to dissolve KPS initiator (3.01 g). Monomer (190 g) was added to the reactor and emulsified by stirring at 450 rpm, and finally initiator solution added. The reaction was left to proceed for 3 h before the temperature was raised to 80 °C and the reactor vessel opened. The reaction was then left to proceed for a further 12 h to remove residual monomer and residual initiator. This seed latex, MMA06, was dialyzed against distilled water for 10 days, over which time conductivity measurements became constant. The dialyzed latex was filtered through glass wool to remove any traces of coagulum. Particle size distributions were measured by the following techniques (average diameters given in parentheses): capillary hydrodynamic fractionation (CHDF, Matec; 85 nm number-average); dynamic light scattering (HPPS, Malvern; 99 nm z average); transmission electron microscopy (TEM; 88 nm number-average), using carbon sputtering. The CHDF value was used in subsequent work.

Seeded Studies: Rates from Dilatometry. The techniques used for obtaining rate data by dilatometry, with both chemical and γ-radiolytic initiation (with both in-source and out-of-source, or relaxation, modes), were as described elsewhere.[14] In the case of MMA, which is appreciably soluble in water, nonideal mixing of monomer and water may not be neglected and the approach of Ballard et al.[15] was used to calculate conversion for such systems. For this purposes, one requires the saturated solubility of monomer in water, $[M]_w^{sat}$ and in latex particles, $[M]_p^{sat}$. The latter value was measured at 50 °C (the temperature used for kinetic experiments) for seed latex MMA06 using the "static swelling" method.[5,15,16] The value so obtained, 6.9 M, is close to that of 6.6 M reported by Ballard et al.[15] All chemically initiated runs were performed with a particle number density $N_p = 4.3 \times 10^{16}$ L^{-1}.

Seeded emulsion polymerization compositions for all γ- and chemically initiated runs at 50 °C are given in Table 1. Polymerization rates were measured by automated dilatometry assuming ideal mixing with the densities of monomer and polymer at 50 °C taken as $d_M = 0.909$ g cm^{-3} and $d_p = 1.226$ g cm^{-3} respectively,[17] the latter being the density of polymer in a monomer solution (applicable to monomer-swollen latex particles). The density of monomer dissolved in water at 50 °C was measured experimentally as 0.981 g cm^{-3}. Final dilatometric conversions were verified by gravimetry to ensure accuracy of the dilatometry procedures. For reasons given elsewhere,[15] for pseudo-bulk systems such as these it is useful to present conversion data as mass rather than as fraction conversion.

Table 1. Details of Seeded Emulsion Polymerizations

	chemically initiated experiments	γ-radiolysis experiments
N_p/L^{-1}	4.3×10^{16}	1.0×10^{17}
seed (MMA06) polymer/g	0.89	0.92
MMA/g	5.25	4.80
AMA-80/g	0.031	0.033
KPS/g	0.004−0.05	−
γ-radiolysis dose rate/Gy h^{-1}	−	146

Table 2. Initiator Concentrations and Initial Pseudo-Steady-State n for Chemically Initiated Runs

run	[KPS]/mM	$\bar{n}_{initial}$
C68	0.10	0.17
C69	0.30	0.26
C73	1.0	0.33
C72	3.0	0.45

Molecular Weight Distributions. Molecular weight distributions were measured for the seed latex polymer and the polymer from latexes produced in four seeded kinetic experiments with potassium persulfate as chemical initiator. The seeded runs were monitored by dilatometry and stopped at the end of interval 2 (i.e., before the disappearance of monomer droplets), rapidly quenched with hydroquinone, and cooled in an ice bath. Samples were prepared by dissolving the dried polymer in tetrahydrofuran at 0.1 wt %. Analyses were carried out using a Shimadzu SEC system fitted with a series of three HT6E Waters columns and a refractive index detector. The molecular weight distribution was determined with Polymer Laboratories Cirrus software. A calibration curve was constructed using a combination of low polydispersity poly(MMA) (Polymer Standards Service, molecular weight range 5.05×10^2 to 2.5×10^6) and polystyrene (Polymer Laboratories, molecular weight range 5.0×10^3 to 1.0×10^7) standards; nonlinearity of this calibration curve was fully taken into account in the data processing. Universal calibration was employed for the polystyrene standards, using the following Mark−Houwink parameters: $K = 14.1 \times 10^{-3}$ mL g^{-1}, $\alpha = 0.7$ for polystyrene; $K = 12.8 \times 10^{-3}$ mL g^{-1}, $\alpha = 0.69$ for poly(MMA). Because a poly(MMA) of very high molecular weight was produced, the polystyrene standards were needed to cover the range of molecular weight of up to 1.0×10^7 and even slightly beyond.

Results

Chemical Initiation: MWD and Rate Data. Table 2 gives initiator concentrations and rate results for chemically initiated runs. Typical rate data are shown in Figure 1, and also the corresponding data for $\bar{n}$, which are related to the rate by

$$\frac{d\hat{x}}{dt} = \frac{k_p [M]_p M_0 N_p V_w}{N_A} \bar{n} \qquad (5)$$

where $\hat{x}$ is the mass of monomer converted, $[M]_p$ the monomer concentration within the particles, and V_w the volume of the water phase. The values of k_p are well established over a wide temperature range for MMA.[18]

Figure 1 and corresponding data for other initiator concentrations all show a rapid attainment of a pseudo-steady state (within ~2 min in Figure 1), whereafter $\bar{n}$ shows an approximate steady state with a slight increase with conversion (acceleration) over interval 2. The reason for this slight increase is well established,[15]

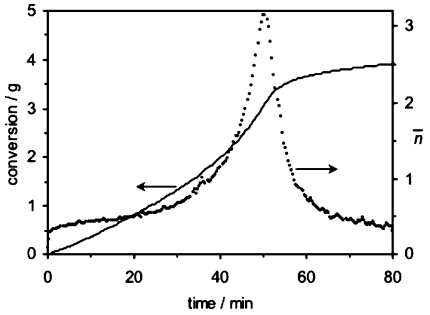

Figure 1. Conversion (line) and $\bar{n}$ (points) as functions of time for a chemically initiated seeded emulsion polymerization of MMA at 50 °C with [KPS] = 1 mM. Interval 2 is from 0 to 17 min.

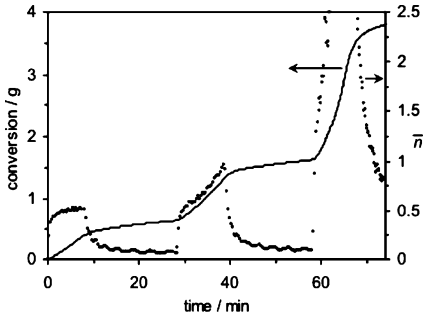

Figure 2. Conversion (line) and $\bar{n}$ (points) as functions of time for a γ-relaxation experiment at 50 °C with γ-radiolysis dose rate of 146 Gy h^{-1}. Interval 2 is from 0 to 30 min.

and will be one of the subjects of a subsequent publication on entry rate coefficients in this system. It is noted that $\bar{n}$ is by no means restricted to a value below $^1/_2$, as indeed expected for a system such as this which falls into the common category of pseudo-bulk kinetics.[15]

Duplicate relaxation experiments were performed; Figure 2 shows some data from an experiment in which two γ-relaxations were performed during the same run. As with chemical initiation, the value of $\bar{n}$ in interval 2 shows a slight acceleration.

The MWDs pertaining to run C69 are shown in Figure 3, first as SEC distributions; the calibration curve is also shown as an inset in this figure. The MWD of the seed polymer was then subtracted from that of the total polymer obtained at the end of run C69. The subtraction took into account the relative amounts of seed and new polymer, following methodology described eslewhere.[19,20] The resulting "pseudo-instantaneous" MWD is that due only to new polymer formed during run C69, which was at 50 °C and only in interval 2, where the monomer concentration corresponds to a weight fraction of polymer $w_p = 0.30$.

Following the discussion given above, this pseudo-instantaneous SEC distribution, $w(\log M)$, is replotted as the number distribution $P(M)$ using eq 3. This is presented as a separate panel in Figure 3. This log-linear plot of $P(M)$ is expected to show an extensive straight-line region. However, it is apparent that this is not the case. Data for all four runs are shown in Figure 4 as both $w(\log M)$ and as ln $P(M)$, in which the remarkably high molecular weights produced by these polymerizations are evident: all the SEC distributions peak at nearly 10^7. Importantly, it will be seen in the following sections that these MWDs are fully consistent with expected kinetic parameter values, i.e., we are confident that the MWDs are correct.

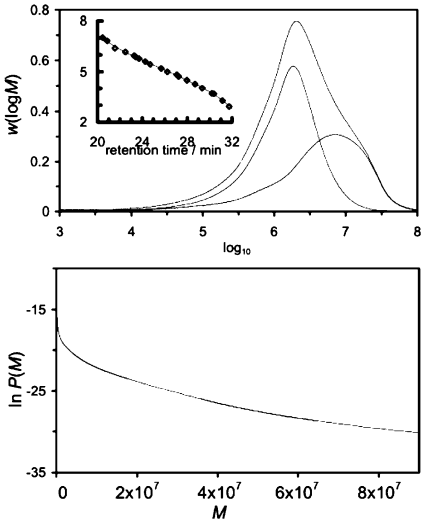

Figure 3. Top panel: SEC distributions from interval 2 seeded emulsion polymerization of MMA at 50 °C with [KPS] = 3×10^{-4} M (run C69): cumulative MWD for total polymer from seeded run (— — —), cumulative MWD of seed (latex MMA06) polymer (- — - — -), and pseudo-instantaneous MWD of new interval 2 polymer (—); the inset shows the calibration curve. Bottom panel: the pseudo-instantaneous data as a ln P plot.

The plots of ln P in Figure 4 all display the same concave-up nonlinearity. Close examination almost all previous studies[7,11,20–27] of ln P reveals significant nonlinearity and also the same concave-up behavior, with the only exception being the essentially linear distributions that have been obtained from some experiments with added chain transfer agent.[28,29]

Nonlinear ln *P* MWD Plots: The Effects of Broadening. Some aspects of the work given in this section have been published in an earlier communication.[30] The expected linearity in pseudo-instantaneous ln P plots seems experimentally to be more honored in the breach than in the observance. It has been suggested that observed nonlinearity may be the result of errors introduced by the GPC baseline subtraction,[31] in the isolation of the new polymer MWD from the seed MWD, and/or the effects of GPC band broadening of the distribution. Consideration of such issues has led to the suggestion that the most accurate value for the true slope of ln P may be obtained by fitting of the region of the ln $P(M)$ distribution corresponding to the peak region of the associated $w(\log M)$ distribution,[11,28,31,32] and that fitting of the highest molecular weight region may be more prone to error.

Because baseline subtraction might be expected to provide error of a random nature, we suggest here that the observation of a concave-up form that seems to almost always be present over a variety of experimental studies provides strong evidence that baseline subtraction is not the fundamental origin of the effect. This suggests that quantitative investigation of band broadening as the origin of the effect is merited − an investigation which is implemented in the present section.

The basic treatment of broadening is well-known (see, e.g., a recent review[10]) and is summarized here. Denote by $S(t)$ the signal from SEC at an elution time t (elution time and elution volume may be used interchangeably). Because of broadening, a perfectly monodisperse standard will not elute over an infinitely narrow elution time, and thus for any input MWD, the signal has

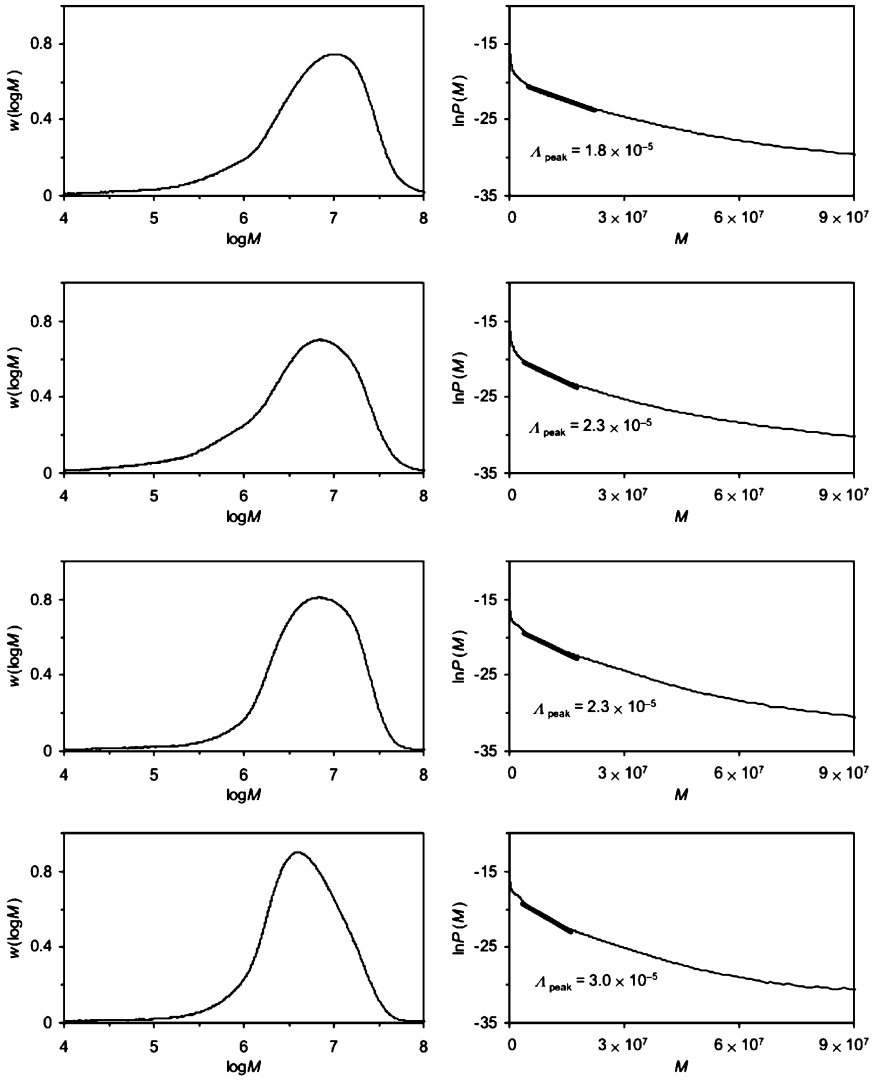

Figure 4. As in Figure 3, for (top to bottom) runs C68, C69, C73, and C72. The slopes Λ of ln *P* at the peak (maximum) in the SEC distributions are also indicated (note that the values of Λ are not those of the actual plots here but are those with respect to degree of polymerization rather than molecular weight—see the definition of eq 4).

contributions from all molecular weights eluting at a given time, expressed as a convolution equation:[33−35]

$$S(t) = \int_0^\infty G(t,M)\, M\, P(M)\, \mathrm{d}M \tag{6}$$

Here the spreading function $G(t,M)$ is the signal that would be obtained at elution time t from a perfectly monodisperse sample with molecular weight M, and the MWD in the integral is chosen to be the weight distribution $M\,P(M)$, because by expressing the convolution in this form it is sometimes adequate for the spreading function to have a simple Gaussian form:[10]

$$G(t,M) = \exp\left(\frac{-(t - t'(M))^2}{2\sigma^2}\right) \tag{7}$$

Here σ is the broadening width and $t'(M)$ the SEC calibration curve: the elution time at which the signal $S(t)$ is a maximum when a perfectly monodisperse sample of molecular weight M is eluted; (of course both the broadening width and the calibration curve depend on the particular SEC column and instrument).

It is well established (for example, as discussed in the review by Baumgarten et al.[10]) that a simple Gaussian broadening function is inadequate for accurate work, and instead more flexible functional forms are preferred, such as the "exponential-Gaussian hybrid" (EGH), defined by[36]

$$G(t,M) = \begin{cases} \dfrac{1}{C}\exp\left(\dfrac{-(t - t'(M))^2}{2\sigma^2 + (t - t'(M))\tau}\right) & 2\sigma^2 + (t - t'(M))\tau > 0 \\ 0 & 2\sigma^2 + (t - t'(M))\tau \le 0 \end{cases} \tag{8}$$

where σ is the standard deviation of the precursor Gaussian, τ is the time constant of the precursor exponential, and C is a normalization constant. A linear calibration curve has the form:

$$\log_{10} M = a - bt', \quad \text{i.e.,} \quad t'(M) = \frac{a}{b} - \frac{1}{b}\log_{10} M \tag{9}$$

The effect of broadening is exemplified in Figure 5, which shows the result of taking the $P(M)$ of eq 4, with the transfer constant k_{tr}/k_p that reported for MMA at

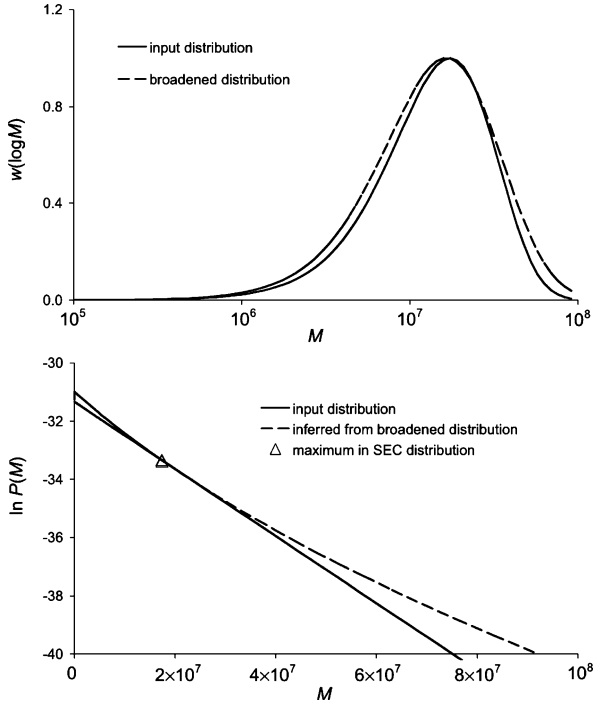

Figure 5. Effects of broadening modeled using eqs 4 and 6−9, presented in the same way as the experimental data of Figures 3 and 4. Parameter values given in text. The ln P plot also shows the point where $w(\log M)$ has its maximum.

50 °C by Stickler and Meyerhoff for a highly purified MMA bulk system ($k_{tr}/k_p = 1.16 \times 10^{-5}$).[37] An EGH spreading function, eq 8, was chosen with parameter values determined[38] in the laboratory of one of the authors (RGG) for aqueous SEC data on linear starch, fitting the SEC distribution to that obtained by capillary electrophoresis (which gives absolute molecular weight distributions). These EGH spreading parameters are $\sigma = 0.23$ min, $a = 19.8$, $b = 0.65$ min^{-1}, and $\tau = -3.85 \times 10^{-4}$ min.

The numerical integration involved in this calculation can be accurately implemented using standard numerical quadrature procedures with a small number of points if the variable of integration in eq 6 is transformed to elution time and integration performed in equal increments of t'.

The results of this model calculation are presented in Figure 5 in the same way as actual data for the present MMA system, except that now the true SEC distribution is compared to the (simulated) broadened one, and the true ln $P(M)$ with that obtained by applying eq 3 to the broadened distribution (but ignoring broadening). We denote the latter by ln P_{broad}. It is apparent that this relatively small, but realistic, broadening preserves the general form of $w(\log M)$, including the maximum, but induces a concave-up curvature in ln P_{broad}. This *qualitative* trend is consistent with many experimental observations. The reason for preserving the maximum is that broadening effects approximately cancel at a maximum (recall that the broadening integrand is proportional to $M\ P(M)$, which has this maximum). The reason for the upward concavity in ln P is also straightforward, arising from the skewness toward both the higher and lower parts beyond the maximum induced by the form of these two functions and the coordinate transformation.

An essential point from this example is that one sees from Figure 5 that, while ln P_{broad} no longer is a straight line, the slope of the ln P_{broad} at the point of the maximum in the SEC distribution is to a good approximation the *same as that of the true* ln P: the broadened ln $P(M)$ slope at the maximum in $w(\log M)$ differs by 9% from that of the exact ln $P(M)$.

These two observations made from Figure 5 are that (1) broadening induces an upward concavity in ln P_{broad} and that (2) the slopes of the true ln P and ln P_{broad} are almost the same at the maximum in $w(\log M)$. Similar close matches are also seen when these model calculations are performed with a wide variety of parameters for both $P(M)$ and $G(t,M)$. Thus, the common observation of upward-concave ln P plots is explained. Second, it suggests that quantitative interpretation of these plots can be done by taking the slope of ln $P(M)$ at the maximum in $w(\log M)$ (as suggested elsewhere for purely empirical reasons[11,28,31]).

We now prove in the following approximate way that the slope of the maximum of ln P from a broadened $w(\log M)$ gives the correct slope of the true ln P. The form of G is taken to be that of eq 7, and the calibration curve to be that of eq 9. Because one expects most of the contribution to the signal at a particular evolution time t to be from a moderate but not large range of molecular weight, it can be assumed that one can approximate the local functional form of $w(\log M)$ by a Gaussian:

$$w(\log M) = M^2\, e^{-(\text{constants})\times M} \approx \exp\left(\frac{-(t'(M))^2}{2s^2}\right) \quad (10)$$

where $t'(M)$ is given by eq 9. While eq 10 is of course not the more complex functional form of the $w(\log M)$ that arises from a linear ln $P(M)$, it furnishes an accurate fit to this more complex functional form in the neighborhood of the maximum in $w(\log M)$. Substituting eqs 7, 9, and 10 into eq 6 and evaluating the integral, one obtains

$$S(t) = \left(\frac{2\pi}{s^{-2} + \sigma^{-2}}\right)^{1/2} \exp\left(\frac{-t^2}{2(s^2 + \sigma^2)}\right) \quad (11)$$

For conventional free-radical polymerizations and typical SEC equipment, it is expected that the width of $w(\log M)$ (i.e., the value of the parameter s that we have assumed fits this distribution locally in eq 10) would be significantly greater than the broadening (i.e., the value of σ). Under these circumstances, one sees that to second order in σ/s, the functional form of $w(\log M) = S(t'(M))$ at the maximum is the same in the true and broadened distributions, including both having the same maxima. Hence the two will have the same slope of the corresponding ln $P(M) = \ln(M^2 S(t'(M)))$.

It is emphasized that this proof requires that broadening be Gaussian in form and significantly less than the width of the distribution. Nevertheless, this approximate result is surprisingly robust. The results in Figure 5 show that this is an excellent approximation with the $w(\log M)$ from an exponential $P(M)$ (which is of course not Gaussian), and with a non-Gaussian, and experimentally realistic, spreading function (the EGH function used for this calculation being taken from a real system in which it was possible to obtain the spreading parameters directly). Similar model calculations with a range of spreading parameters all show that

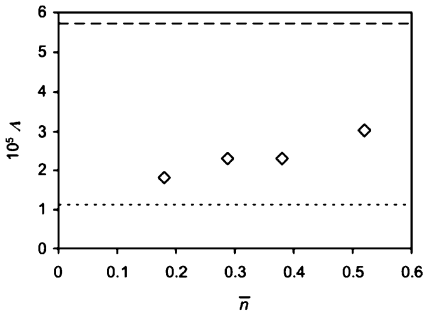

Figure 6. Points: values of Λ, from the data of Figure 4, as a function of $\bar{n}$ for chemically initiated seeded emulsion polymerizations of MMA at 50 °C over a range of initiator concentrations. The values of k_{tr}/k_p from Whang et al.[39] (– – –) and from Stickler and Meyerhoff[37] (.....) are also shown.

the slope of the broadened ln P at the SEC maximum is an excellent approximation to the input value of the true ln P.

Although there are a number of means of taking broadening into account by deconvolution (see the review of Baumgarten et al.[10]), these all require some a priori knowledge of the broadening applicable to the particular experimental system in use. Such information can be very hard to obtain. It has been pointed out[30] that this can be obviated in cases where a simple exponential $P(M)$ is anticipated (especially MWDs obtained in the presence of excess transfer agent in free-radical systems) by the simple procedure of taking the slope of ln P_{broad} at the maximum of $w(\log M)$. Moreover, if one were to perform SEC measurements on a sample which one knew to have a single-exponential $P(M)$, such as that obtained with excess of transfer agent, this provides a means of quantifying the broadening in the SEC system used for the measurements.

Obtaining Rate Coefficients from SEC and Rate Data. MWDs. The starting point of analysis for the SEC data is the result deduced by Clay et al. in eq 4, which implies that a plot of the slope Λ of ln $P(M)$ as a function of M against $\bar{n}$ should be linear, if $\langle k_t \rangle$ is similar for the conditions of each data point, with intercept k_{tr}/k_p and the slope being a quantity from which $\langle k_t \rangle$ can be inferred. The data of Figure 4 are for systems which are all in Interval 2, i.e., at the same weight-fraction of polymer w_p. Because simulations[9,11] suggest that $\langle k_t \rangle$ should not be strongly dependent on initiator concentration (for the range used here), one expects from eq 4 that a plot of Λ against $\bar{n}$ should show approximately linear behavior; the actual behavior is shown in Figure 6. In view of the discussion in the preceding section, the value of Λ for this purpose was taken to be the slope of ln P at the molecular weight at which $w(\log M)$ is a maximum. It is noted that although (as shown in Figure 3) the standards used in calibration go only to $M \sim 10^7$, these maxima are never more than slightly above this value, and moreover there is (as also seen in Figure 3) no evidence that these data are anywhere near the exclusion limit of the columns. Hence the MWD at the maximum in the SEC distributions are regarded as being free from any artifacts from extrapolation of the calibration curve and from the exclusion limit of the column. Also shown are two values from the literature for k_{tr}/k_p at 50 °C: that of Stickler and Meyerhoff, using essentially the Mayo method for a highly purified MMA bulk system,[37] and that of Whang et al.,[39] who used what is essentially eq 4 to infer this quantity from early SEC data in MMA emulsion polymerization. The latter value, and a similar value obtained in a similar ln P study by Kukulj et al.,[21] are both much higher than that of Stickler and Meyerhoff, a discrepancy which may arise from the presence of some adventitious impurities in the emulsion studies. Equation 4 is used together with a linear fit to the Λ data of Figure 6 to infer rate coefficients. The intercept gives $k_{tr}/k_p = (1.22 \pm 0.25) \times 10^{-5}$ M^{-1} s^{-1}. This is remarkably close to the Stickler–Meyerhoff value at 50 °C: $(1.16 \pm 0.2) \times 10^{-5}$ M^{-1} s^{-1}. The slope gives the value of $\langle k_t \rangle$ as $(1.7 \pm 0.3) \times 10^5$ M^{-1} s^{-1}, which will later be compared to the value of $\langle k_t \rangle$ from the γ relaxation data.

Mayo method. There has been considerable discussion in the literature[11,21,28,31,32,40,41] of the similarities and differences (not to mention the relative advantages and disadvantages) between the ln $P(M)$ slope methodology used above and the more traditional Mayo method for determining k_{tr} and $\langle k_t \rangle$. It is therefore of interest to complement the above analysis with the approach of Mayo, which uses:

$$\frac{1}{\bar{X}_n} = \frac{k_{tr}}{k_p} + \frac{(1+\lambda)\langle k_t \rangle R_{pol}}{(k_p[M]_p)^2 N_A V_s} \qquad (12)$$

where $\bar{X}_n$ = number-average degree of polymerization, λ = fraction of termination occurring by disproportionation (with $\lambda \approx 1$ assumed here for MMA[42,43]), and $R_{pol} = k_p[M]_p\bar{n}$ in the present instance. The similarity between these two methods is immediately evident upon comparison of eqs 4 and 12, and in practical terms the Mayo approach is identical to that used above. In principle a plot of $1/\bar{X}_n$ vs $R_{pol}/(N_A V_s)$ may be used to infer a value of $\langle k_t \rangle$, if $\langle k_t \rangle$ does not change, a fact which may limit the accuracy of this approach, just as it does the ln P approach above—the essentially identical nature of the equations shows that if a varying $\langle k_t \rangle$ affects one approach, then it must equally affect the other. However since $\langle k_t \rangle$ should not be strongly dependent on initiator concentration (for the range used here), one expects a Mayo plot to be linear, and certainly the value of $1/\bar{X}_n$ must converge to k_{tr}/k_p in the transfer limit. Thus, it may still be possible to obtain accurate values for k_{tr}/k_p under transfer-controlled conditions.

Values of $1/\bar{X}_n$ may be most simply obtained for experimental $P(M)$ distributions. However, the value of $\bar{M}_n$ is considerably more sensitive to SEC uncertainties than the weight-average molecular weight $\bar{M}_w$,[31] and we here assume (as have others[28,44]) a value for the polymer polydispersity of $\bar{M}_w/\bar{M}_n = 2$. It is pointed out that since a polymer polydispersity index of 2 is characteristic of MWDs for dead chains formed by transfer or termination by disproportionation, the above assumption is likely to be a good one for MMA systems irrespective of whether transfer-controlled conditions hold. The plot of $1/\bar{X}_n$ against R_{pol} so obtained is essentially the same as Figure 6, and therefore it is not presented. The values obtained from the slope and intercept of a linear fit to these data give $\langle k_t \rangle = 7.5 \times 10^4$ M^{-1} s^{-1}, less than that obtained from the ln P approach and closer to the value from rate measurements given below, while the value $k_{tr}/k_p = 1.27 \times 10^{-5}$ M^{-1} s^{-1} is very similar to that from both the ln P method and from Stickler and Meyerhoff.

Termination Rate Coefficients from Relaxation Data. The γ-radiolysis relaxation data were analyzed by integrating eq 2 and then eq 5 to give

$$\bar{n} = \bar{n}_f \frac{Q\exp(2\delta t) - 1}{Q\exp(2\delta t) + 1} \tag{13}$$

$$\hat{x} = \frac{k_p[M]_p M_0 N_p V_w}{N_A c}\,[\ln|Qe^{\delta t} + \exp^{-\delta t}| - \ln|Q+1|] \tag{14}$$

Here $c = \langle k_t\rangle/N_A V_s$, $Q = (\bar{n}_f + \bar{n}_i)/(\bar{n}_f\bar{n}_i)$, $\delta = 2c\bar{n}_f$, and $\bar{n}_f = (\rho/2c)^{1/2}$. $\bar{n}_i$ and $\bar{n}_f$ denote the initial and final steady-state values of $\bar{n}$ respectively. These results have been presented elsewhere,[15] but without the modulus functions, and consequently in a form that is limited in its use. The form given above (including moduli) is a general result applicable to the kinetics of both a γ-insertion or γ-relaxation, and also to the approach to steady-state for a chemically initiated polymerization. In the γ-relaxation case, the value of ρ is that from entry of spontaneously generated radicals only, ρ_{spont}, and the final value of $\bar{n}$ is that from spontaneous polymerization, $\bar{n}_{spont}$.

Values for ρ_{spont} and $\langle k_t\rangle$ were obtained by nonlinear least-squares fitting of eq 14 to the experimental conversion−time data obtained immediately after removal of the system from the γ-source; this resulting two-parameter fit closely matched the data. These values are $\langle k_t\rangle = (1.9 \pm 0.1) \times 10^4$ M^{-1} s^{-1}, $\bar{n}_{spont} = 0.074 \pm 0.007$, $\rho_{spont} = (1.5 \pm 0.1) \times 10^{-4}$ s^{-1} (the experimental uncertainties are estimated from the two measurements). Equations 13 and 14 assume a constant value of $[M]_p$. Since $\langle k_t\rangle$ will be affected by the viscosity of the latex particle interior and therefore sensitive to changes in the weight fraction of polymer (w_p) inside the particles, the only data used for analysis of radical loss kinetics were those from the first relaxation in each experiment. These commenced in Interval 2, where the values of $[M]_p$ (6.9 M) and consequently of w_p (0.30) are approximately constant due to the presence of excess monomer. The values of $\langle k_t\rangle$ and ρ_{spont} are in acceptable agreement with those measured in Interval 2 by Ballard et al.:[15] $\langle k_t\rangle = (3.8 \pm 1.0) \times 10^{-4}$ M^{-1} s^{-1} and $\rho_{spont} = (2.5 \pm 2.0) \times 10^{-4}$ s^{-1}. The value of $\langle k_t\rangle$ here differs from that of Ballard et al. only by a factor of about 1.5, which is a very small difference given the usual spread noted in the literature values for $\langle k_t\rangle$.[12] Moreover, it is noted that the data of Ballard et al. were subject to quite significant scatter and that the present experimental apparatus has much greater precision and accuracy than that available to Ballard et al.

It is seen that this value of $\langle k_t\rangle$ from the relaxation data is a factor of ~4 smaller than that inferred from the MWD data using the Mayo method, which in turn is a factor of ~2 smaller than that from the ln *P*. Theory is now used to investigate this large discrepancy.

Theory for Rate Coefficients. The data were modeled using a standard treatment[9,45−51] for rates and MWDs in free-radical polymerization, assuming that termination is diffusion-controlled. In brief, one solves the radical balance equations for the n_i:

$$\frac{dn_1}{dt} = \rho + k_{tr}[M]_p\sum_{j=2}^{\infty} n_j - k_p{}^1[M]_p n_1 - 2n_1\sum_{j=1}^{\infty} c_{1j}n_j \tag{15}$$

$$\frac{dn_2}{dt} = k_p{}^1[M]_p n_1 - k_p[M]_p n_2 - k_{tr}[M]_p n_2 - 2n_2\sum_{j=1}^{\infty} c_{2j}n_j \tag{16}$$

$$\frac{dn_i}{dt} = k_p[M]_p(n_{i-1} - n_i) - k_{tr}[M]_p n_i - 2n_i\sum_{j=1}^{\infty} c_{ij}n_j,\ i > 2 \tag{17}$$

$$c_{ij} = \frac{k_t^{ij}}{N_A V_s} \tag{18}$$

$$k_t^{i,j} = \frac{1}{2}k_t^{1,1}(i^{-e} + j^{-e}) \tag{19}$$

The methods used for numerical solution of these equations have been given elsewhere.[9,45−51] We assume the following parameter values for MMA at 50 °C: the rate coefficient for propagation of a monomeric radical $k_p{}^1 = 15\ k_p$,[5,52−55] $e = 1.26$ (which is the exponent predicted at $w_p = 0.30$ by an empirical "universal" scaling law fitted to a range of data on diffusion of oligomers up to degree of polymerization 10 in a wide range of monomer/polymer mixtures),[56,57] the Stickler−Meyerhoff[37] value of $k_{tr} = 1.1 \times 10^{-5}$ $k_p = 7.0 \times 10^{-3}$ M^{-1} s^{-1} (where $k_p = 649$ M^{-1} s^{-1} is the IUPAC-recommended value[18]). The reaction−diffusion contribution to the rate coefficients[58] can be included but makes no difference in this low-w_p regime. The value of $k_t{}^{1,1}$ was treated as an adjustable parameter to fit the γ-relaxation data, yielding a value of 5.1×10^8 M^{-1} s^{-1} for this quantity. A different fit was also performed by specifying a crossover chain length X_c at which the scaling law exponent changes from the value predicted from the empirical "universal" value to the reptation limit of 2; choosing $X_c = 10$ resulted in a fitted value of 8.5×10^8 M^{-1} s^{-1} for $k_t.{}^{1,1}$ A number of other changes in the fitting procedure resulted in similarly small changes in $k_t.{}^{1,1}$

The value of $k_t{}^{1,1}$ can be predicted a priori under the assumption of diffusion-controlled termination[9,45−51] as

$$k_t^{1,1} = 2\pi\sigma_{rad}p_{spin}(D_M + D_M)N_A \tag{20}$$

Here σ_{rad} = interaction radius for radical−radical reaction (taken as 3.0 Å[46]), p_{spin} = probability of radical reaction based on spin alignments (taken as 0.25[46]), and D_M is the diffusion coefficient for a monomer molecule in a latex particle, used to approximate that of a chemically similar monomeric radical (taken as 1.12×10^{-9} m^2 s^{-1} [56]). The value of $k_t{}^{1,1}$ so obtained is 6.4×10^8 M^{-1} s^{-1}, which is remarkably close to that obtained from fitting of γ-relaxation data above. In essence this means that the γ-relaxation termination kinetics are fully in accord with the a priori expectation, suggesting that the termination model that has been used here in modeling is close to the physical truth.

Prediction of MWD Data. The same equations, and the value of $k_t{}^{1,1}$ fitted to the γ relaxation data above, are now used to predict the full MWD obtained with chemical initiator. The MWD data were obtained with

Table 3. Experimental and Calculated Values of the Slope of ln $P(M)$

persulfate concentration/mM	0.10	0.30	1.0	3.0
experimental Λ (from slope of ln P at maximum in $w(\log M)$)	1.8×10^{-5}	2.3×10^{-5}	2.3×10^{-5}	3.0×10^{-5}
Λ from simulated ln P	2.4×10^{-5}	2.4×10^{-5}	2.5×10^{-5}	2.6×10^{-5}
Λ from ln P obtained from simulated broadened $w(\log M)$ at maximum in simulated broadened $w(\log M)$	2.1×10^{-5}	2.4×10^{-5}	2.4×10^{-5}	2.6×10^{-5}

persulfate as chemical initiator, and modeling of the slope of ln P, using eq 4,[9] thus requires the inclusion of a model for the entry rate coefficient ρ, for which we use the so-called "Maxwell−Morrison" model.[59] This assumes that radical entry into particles is by aqueous-phase propagation to a critical degree of polymerization z, and that only radicals of this degree of polymerization may enter; propagation to a z-mer is in competition with aqueous-phase termination. Using the Maxwell-Morrison semiempirical model for the value of z, a model based on the free energy of hydration of sulfate-ended oligomers, predicts $z \sim 4-5$ for the present MMA system; in turn, this predicts 100% initiator efficiency.

Modeling the radical distribution as thus described predicts that $\langle k_t \rangle$ for the present conditions is only very weakly dependent on initiator concentration (and hence also on the assumptions made in modeling the entry rate coefficient). This is implicit in the values of Λ in Table 3 from the simulations: the predicted Λ increases almost negligibly with increasing initiator concentration, implying that the MWD is transfer-dominated (see eq 4), and thus that termination is transfer-dominated, and thus that $\langle k_t \rangle$ is essentially constant. Table 3 also shows the experimental values of the slope of ln P measured at the value of M at the peak in the observed $w(\log M)$.

The simulated MWDs were then compared with experiment by taking broadening into account. To do this completely correctly, it would be necessary to determine the spreading function for the particular SEC setup used here. A method for doing this has recently been deduced,[30] which enables one to find $G(t,M)$ without making assumptions such as this being a Gaussian with constant spreading function, which is known to be inaccurate.[10] However, for the present purpose of understanding the effects of broadening semiquantitatively, this rather complex experimental procedure[30] was not implemented, and instead a simple Gaussian spreading function was assumed, as encapsulated in eqs 6 and 7. In the present case a nonlinear calibration curve was found experimentally, for which the slope b (eq 9) varied over 0.3−0.65 min^{-1} over the range of elution volumes spanned by our poly(MMA) samples. An estimate for the standard deviation of the Gaussian broadening function, σ, was obtained using the SEC traces of the low-polydispersity molecular weight standards used in the GPC calibration. Equation 7 was fitted to the SEC traces of the five highest molecular weight standards (which span the relevant range of elution volumes) and a mean value of $\sigma = 0.4$ min was determined. On the basis of these estimates it is reasonable to expect a value of σb in the range of 0.12−0.26 for the GPC setup used here. The effect of broadening with a range of σb is shown for 0.3 mM persulfate in Figure 7. It is evident that σb as large as 0.45 is needed to obtain close agreement between the experimental and (broadened) simulation MWDs. While this represents a moderately high extent of broadening (but still much less than that of the experimental $w(\log M)$), there is some evidence[10] that SEC broadening does increase as molecular weight increases, and the molecular weights in the present investigation are extremely large.

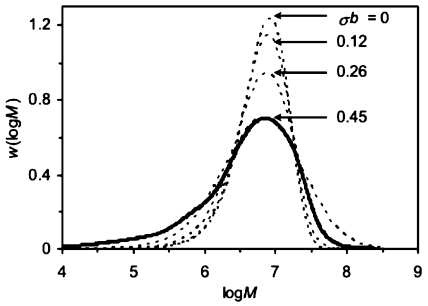

Figure 7. Effect of Gaussian broadening on simulated instantaneous $w(\log M)$ for a seeded emulsion polymerization of MMA at 50 °C with [KPS] = 3×10^{-4} M; MWDs simulated (dashed lines) with increasing broadening applied using values of σ b = 0, 0.12, 0.26, and 0.45 as indicated; solid line: experimental MWD (run C69).

For situations where the broadening is much less, for example the use of a high-quality SEC setup with lower molecular weights, there will still be appreciable broadening, as shown by the $\sigma b = 0.12$ results of Figure 7. Thus, it can never be disadvantageous to apply the procedure suggested here: where errors can be eliminated, they should be.

In view of $\sigma b = 0.45$ being questionably large, the expected upper bound of 0.26 was used for further calculations: all MWD simulation data have been broadened with $\sigma b = 0.26$ and are compared with experiment in Figure 8. It is seen that experiment is adequately reproduced with $\sigma b = 0.26$. The values of Λ of the broadened simulated MWDs at the SEC maximum are given in Table 3. It should be noted that the use of a single value for σb in all simulations implicitly assumes that the extent of broadening is uniform over the range of conditions used, and thus does not allow for, e.g., a dependence of σb on polymer molecular weight. However, given that the overall nature of the MWDs is seen to vary only slightly under the present conditions (see Figure 8), this assumption is unlikely to significantly affect any kinetic inferences made.

The very acceptable accord obtained between experiment and modeling means that reliable inferences can be drawn from examination of the details of the model for this particular system. The most important inferences are that (a) the dominant *chain-stopping* event is transfer to monomer, i.e., that the MWDs are transfer-controlled, while (b) the dominant *radical los*s event is short−long termination between a rapidly diffusing short radical resulting from transfer and an immobile long one. However, radical activity is maintained over many cycles of transfer, i.e., not every transfer event results in termination, and hence the termination rate coefficient is not simply that for transfer.

A single parameter value, k_{tr}, was varied in obtaining the simulation results of Figure 8; its effect is to shift the SEC distributions (i.e., change their central position), with it having no effect on width. The best-fit value was found to be $k_{tr} = 2.3 \times 10^{-5}$ $k_p = 1.5 \times 10^{-2}$ M^{-1} s^{-1}. This value is about a factor of 2 higher than

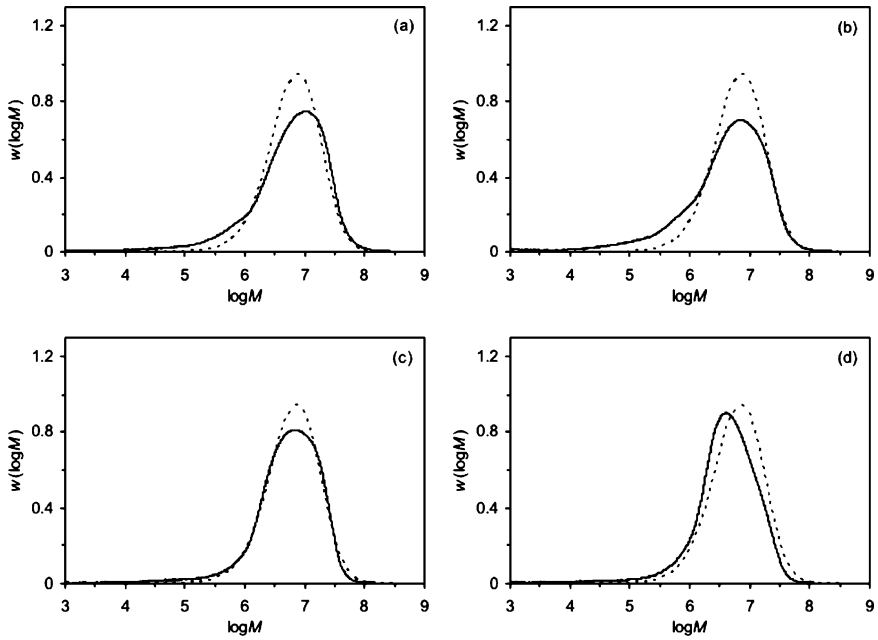

Figure 8. Effect of Gaussian broadening ($\sigma b = 0.26$) on simulated instantaneous MWDs for chemically initiated seeded emulsion polymerizations of MMA at 50 °C; experimental (solid lines) and simulated (dashed lines) MWDs for a range of initiator concentrations: [KPS] = 1×10^{-4} M (a), 3×10^{-4} M (b), 1×10^{-3} M (c), and 3×10^{-3} M (d).

the Stickler−Meyerhoff value of $k_{tr}/k_p = 1.1 \times 10^{-5}$ and a factor of 2 lower than the Whang et al. value. Because the value of 2.3×10^{-5} has been obtained by fitting the entire MWD distribution including broadening (see Figure 8), as opposed to fitting of Λ or $\bar{X}_n$ only (as carried out above), it is recommended as the best value from the present work. The observation that the present k_{tr} value is slightly higher than the Stickler−Meyerhoff value could reflect either SEC differences or that the present emulsion systems are slightly more impure than Stickler and Meyerhoff's ultraclean bulk systems. The fact that the present value is so close to the Stickler−Meyerhoff value is supportive of both values, and reflects that the chain-stopping kinetics are indeed the same in these very different systems: intermediate-conversion emulsion polymerization with chemical initiator as opposed to low-conversion bulk polymerization with no added initiator.

It is noted that molecular weights in this system are high. However, unlike styrene,[11,60] this is not due to the suppression of termination that accompanies radical compartmentalization in a zero-one emulsion system.[5] The present MMA system is pseudo-bulk, and thus has a frequency of termination and thus polymer molecular weights similar to those in a bulk system. The explanation for the high molecular weights measured here is transfer control.

Some insight has now been gained into why the plots of experimental Λ against $\bar{n}$, Figure 6, and of $1/\bar{X}_n$ against R_{pol} (not shown), yielded estimates of $\langle k_t \rangle$ that are too high. The reason is that chain-stopping is transfer-dominated, which means that the transfer contribution to Λ and $\bar{X}_n$ completely dominates that from termination (see eqs 4 and 12). This is evident from the values of Λ reported in Table 3: the unbroadened simulation values are barely above the input $k_{tr}/k_p = 2.3 \times 10^{-5}$. Thus, the slope of a Mayo plot or a plot of Λ against $\bar{n}$ is in the present case dominated by experimental scatter, and so it is impossible to obtain $\langle k_t \rangle$ accurately—in fact the more credible approach is just to regard the experimental $1/\bar{X}_n$ or Λ values as k_{tr}/k_p estimates (see experimental values of Λ in Table 3). Further, by comparing the broadened and unbroadened values of Λ from simulations, it is evident that broadening introduces a greater variation into the Λ values, which explains why the plots overestimate $\langle k_t \rangle$.

Conclusions

A long-standing mystery in examination of the number MWDs in free-radical polymerization has been that, while theory predicts that the instantaneous number distribution should be a single exponential in M (i.e., ln P should be linear in M), experiment has always shown significant nonlinearity with a concave-up ln P. It is now apparent that this can be explained by band broadening in SEC. Moreover, the slope of the true "unbroadened" ln P can be obtained from the observed (experimentally broadened) one by taking the slope of the broadened ln P_{broad} at the value of molecular weight corresponding to the peak molecular weight in the experimental instantaneous SEC distribution; this is because broadening effects cancel at this turning point, at least to a good approximation.

The theory and experiment presented here for MMA make it apparent that in the not uncommon case where termination is transfer-dominated, the plot of the slope of ln P against rate suggested by Clay et al.[11,60] as a means of obtaining termination rate coefficients from experiment cannot be utilized.

The relaxation rate data and MWD data for MMA together are successfully modeled using the diffusion-controlled model for termination, with the chain-length dependence of the termination rate coefficients being modeled with the empirical scaling law deduced from pulsed-field-gradient NMR data for oligomer diffusion coefficients.[56,57] The good agreement found here quantitatively supports the notion that the Smoluchowski equation provides a good foundation for modeling termination kinetics in the present system. It also means

that, to good approximation, the values of $\langle k_t \rangle$ required to fit experimental kinetic data may be predicted entirely from first principles based on the model for chain length dependent termination used here. The modeling, and the qualitative trends observed experimentally, imply that the rate-determining step in *chain stoppage* (i.e., what controls the MWD) is transfer; the rate-determining step in *radical loss* is diffusion (of a short chain formed by transfer to monomer).

Acknowledgment. The support of a New Zealand Foundation for Research Science and Technology Bright Future Scholarship is gratefully acknowledged, as is the support of the P. A. Rolfe Scholarship Fund and also a Shirtcliffe Fellowship. Jeffrey Castro is thanked for helpful discussions on band broadening, and David Sangster for helpful advice on γ-radiolysis measurements. Dr. Chris Ferguson is thanked for performing the SEC measurements. The support of the Australian Institute for Nuclear Science and Technology is greatly appreciated. The Key Centre for Polymer Colloids is established and supported under the Australian Research Council's Research Centres Program.

References and Notes

(1) Buback, M.; Egorov, M.; Gilbert, R. G.; Kaminsky, V.; Olaj, O. F.; Russell, G. T.; Vana, P.; Zifferer, G. *Macromol. Chem. Phys.* **2002**, *203*, 2570−2582.
(2) Benson, S. W.; North, A. M. *J. Am. Chem. Soc.* **1962**, *84*, 935−940.
(3) Rizzardo, E.; Chiefari, J.; Chong, Y. K.; Ercole, F.; Krstina, J.; Jeffery, J.; Le, T. P. T.; Mayadunne, R. T. A.; Meijs, G. F.; Moad, G.; Moad, C. L.; Thang, S. H. *Macromol. Symp.* **1999**, *143*, 291−307.
(4) Matyjaszewski, K. *ACS Symp. Ser.* **1998**, *685*, 2−30.
(5) Gilbert, R. G. *Emulsion Polymerization: A Mechanistic Approach*; Academic: London, 1995.
(6) Lansdowne, S. W.; Gilbert, R. G.; Napper, D. H.; Sangster, D. F. *J. Chem. Soc., Faraday Trans. 1* **1980**, *76*, 1344−1355.
(7) Christie, D. I.; Gilbert, R. G.; Congalidis, J. P.; Richards, J. R.; McMinn, J. H. *Macromolecules* **2001**, *34*, 5158−5168.
(8) Shortt, D. W. *J. Liquid Chromatogr.* **1993**, *16*, 3371−3391.
(9) Clay, P. A.; Gilbert, R. G. *Macromolecules* **1995**, *28*, 552−569.
(10) Baumgarten, J. L.; Busnel, J. P.; Meira, G. R. *J. Liquid Chromatogr. Relat. Technol.* **2002**, *25*, 1967−2001.
(11) Clay, P. A.; Christie, D. I.; Gilbert, R. G., In *Advances in Free-Radical Polymerization*; Matyjaszewski, K., Ed.; American Chemcal Society: Washington DC, 1998; Vol. 685, pp 104−119.
(12) Buback, M.; Egorov, M.; Gilbert, R. G.; Kaminsky, V.; Olaj, O. F.; Russell, G. T.; Vana, P.; Zifferer, G. *Macromol. Chem. Phys.* **2003**, *203*, 2570−2582.
(13) Moad, G.; Solomon, D. H. *The Chemistry of Free Radical Polymerization*; Pergamon: Oxford, England, 1995.
(14) van Berkel, K. Y.; Russell, G. T.; Gilbert, R. G. *Macromolecules* **2003**, *36*, 3921−3931.
(15) Ballard, M. J.; Napper, D. H.; Gilbert, R. G. *J. Polym. Sci., Polym. Chem. Ed.* **1984**, *22*, 3225−3253.
(16) Halnan, L. F.; Napper, D. H.; Gilbert, R. G. *J. Chem. Soc., Faraday Trans. 1* **1984**, *80*, 2851−2865.
(17) Eastmond, G. C. Makromol. Chem., Macromol. Symp. **1987**, 10−11, 71−87.
(18) Beuermann, S.; Buback, M.; Gilbert, R. G.; Hutchinson, R. A.; Klumperman, B.; Olaj, F. O.; Russell, G. T.; Schweer, J. *Macromol. Chem. Phys.* **1997**, *198*, 1545−1560.
(19) Cunningham, B. F.; Mahabadi, H. K. *Macromolecules* **1996**, *29*, 835−841.
(20) Clay, P. A.; Gilbert, R. G.; Russell, G. T. *Macromolecules* **1997**, *30*, 1935−1946.
(21) Kukulj, D.; Davis, T. P.; Gilbert, R. G. *Macromolecules* **1998**, *31*, 994−999.
(22) Miller, C. M.; Clay, P. A.; Gilbert, R. G.; El-Aasser, M. A. *J. Polym. Sci., Polym. Chem. Ed.* **1997**, *35*, 989−1006.
(23) Zaragoza-Contreras, E. A.; Navarro-Rodriguez, D.; Maldonado-Textle, H. *J. Appl. Polym. Sci.* **2002**, *84*, 1513−1523.
(24) Quadir, M. A.; Snook, R.; Gilbert, R. G.; DeSimone, J. M. *Macromolecules* **1997**, *30*, 6015−6023.
(25) Maeder, S.; Gilbert, R. G. *Macromolecules* **1998**, *31*, 4410−4418.
(26) Pabon, M.; Selb, J.; Candau, F.; Gilbert, R. G. *Polymer* **1999**, *40*, 3101−3106.
(27) Monteiro, M. J.; Subramaniam, N.; Taylor, J. R.; Pham, B. T. T.; Tonge, M. P.; Gilbert, R. G. *Polymer* **2001**, *42*, 2403−2411.
(28) Heuts, J. P. A.; Davis, T. P.; Russell, G. T. *Macromolecules* **1999**, *32*, 6019−6030.
(29) Vidal, F.; Guyot, A.; Gilbert, R. G. *Macromol. Chem. Phys.* **1996**, *197*, 1835−1840.
(30) Castro, J. V.; van Berkel, K. Y.; Russell, G. T.; Gilbert, R. G. *Aust. J. Chem.* **2005**, *58*, 178−181.
(31) Moad, G.; Moad, C. L. *Macromolecules* **1996**, *29*, 7727−7733.
(32) Suddaby, K. G.; Maloney, D. R.; Haddleton, D. M. *Macromolecules* **1997**, *30*, 702−713.
(33) Tung, L. H. *J. App. Polym. Sci.* **1966**, *10*, 375−385.
(34) Tung, L. H. *J. App. Polym. Sci.* **1966**, *10*, 1271−1283.
(35) Tung, L. H.; Moore, J. C.; Knight, G. W. *J. App. Polym. Sci.* **1966**, *10*, 1261−1270.
(36) Lan, K.; Jorgenson, J. W. *J. Chromatogr., A* **2001**, *915*, 1−13.
(37) Stickler, M.; Meyerhoff, G. *Makromol. Chem.* **1978**, *179*, 2729−2745.
(38) Castro, J. V.; Ward, R. M.; Gilbert, R. G.; Fitzgerald, M. A. Submitted for publication.
(39) Whang, B. C. Y.; Ballard, M. J.; Napper, D. H.; Gilbert, R. G. *Aust. J. Chem.* **1991**, *44*, 1133−1137.
(40) Heuts, J. P. A.; Clay, P. A.; Christie, D. I.; Piton, M. C.; Hutovic, J.; Kable, S. H.; Gilbert, R. G. *Prog. Pacific Polym. Sci.; Proc.* **1994**, *3*, 203−216.
(41) Christie, D. I.; Gilbert, R. G. *Macromol. Chem. Phys.* **1996**, *197*, 403−412.
(42) Zammit, M. D.; Davis, T. P.; Haddleton, D. M. *Macromolecules* **1996**, *29*, 492−494.
(43) Zammit, M. D.; Davis, T. P.; Haddleton, D. M.; Suddaby, K. G. *Macromolecules* **1997**, *30*, 1915−1920.
(44) Kukulj, D.; Davis, T. P. *Macromolecules* **1998**, *31*, 5668−5680.
(45) Russell, G. T. *Macromol. Theory Simul.* **1994**, *3*, 439−468.
(46) Russell, G. T. *Macromol. Theory Simul.* **1995**, *4*, 497−517.
(47) Russell, G. T. *Macromol. Theory Simul.* **1995**, *4*, 519−548.
(48) Russell, G. T. *Macromol. Theory Simul.* **1995**, *4*, 549−576.
(49) Russell, G. T. *Aust. J. Chem.* **2002**, *55*, 399−414.
(50) Russell, G. T.; Gilbert, R. G.; Napper, D. H. *Macromolecules* **1992**, *25*, 2459−2469.
(51) Russell, G. T.; Gilbert, R. G.; Napper, D. H. *Macromolecules* **1993**, *26*, 3538−3552.
(52) Heuts, J. P. A.; Radom, L.; Gilbert, R. G. *Macromolecules* **1995**, *28*, 8771−8781.
(53) Moad, G.; Rizzardo, E.; Solomon, D. H.; Beckwith, A. L. J. *Polym. Bull. (Berlin)* **1992**, *29*, 647−652.
(54) Gridnev, A. A.; Ittel, S. D. *Macromolecules* **1996**, *29*, 5864−5874.
(55) Willemse, R. X. E.; Staal, B. B. P.; van Herk, A. M.; Pierik, S. C. J.; Klumperman, B. *Macromolecules* **2003**, *36*, 9797−9803.
(56) Griffiths, M. C.; Strauch, J.; Monteiro, M. J.; Gilbert, R. G. *Macromolecules* **1998**, *31*, 7835−7844.
(57) Strauch, J.; McDonald, J.; Chapman, B. E.; Kuchel, P. W.; Hawkett, B. S.; Roberts, G. E.; Tonge, M. P.; Gilbert, R. G. *J. Polym. Sci., Part A: Polym. Chem. Ed.* **2003**, *41*, 2491−2501.
(58) Russell, G. T.; Napper, D. H.; Gilbert, R. G. *Macromolecules* **1988**, *21*, 2133−2140.
(59) Maxwell, I. A.; Morrison, B. R.; Napper, D. H.; Gilbert, R. G. *Macromolecules* **1991**, *24*, 1629−1640.
(60) Scheren, P. A. G. M.; Russell, G. T.; Sangster, D. F.; Gilbert, R. G.; German, A. L. *Macromolecules* **1995**, *28*, 3637−3649.

MA048027G